

POLIMERY

CZASOPISMO POŚWIĘCONE CHEMII, TECHNOLOGII I PRZETWÓRSTWU POLIMERÓW

Reinforcement of epoxy resin/carbon fiber composites by carboxylated carbon nanotubes: a dynamic mechanical study

Hamed Nazarpour-Fard¹⁾, Kurosh Rad-Moghadam^{1),*)}, Farhad Shirini¹⁾,
Mohammad Hosain Beheshty²⁾, Gholam Hosein Asghari²⁾

DOI: dx.doi.org/10.14314/polimery.2018.4.1

Abstract: The composites of epoxy resins reinforced with unidirectional carbon fibers were prepared *via* hot pressing of carbon fiber prepregs. Multiwall carbon nanotubes (MWCNT) derivatives [parent CNTs, low carboxylated CNTs (LCCNTs) and higher carboxylated CNTs (HCCNTs)] were incorporated into the epoxy resin/carbon fiber (E/C) composite. Interestingly, remarkable modifications as consequences of homogeneous dispersion of CNTs in E/C matrix and prevention of void formation within the composite were achieved by using carboxylated CNTs. The dynamic mechanical analysis (DMA) showed improved glass transition temperature (T_g) and storage modulus of the resulting E/C/HCCNT composite. The master curves of storage modulus were constructed for the samples using the Vogel-Fulcher-Tammann (VFT) and Williams-Landel-Ferry (WLF) equations as well as the time-temperature superposition principle (TTS). The apparent activation energies of molecular rearrangements were calculated at different temperatures based on the numerical derivatives and WLF equations. The experimental results indicate that COOH content of CNTs can have a remarkable effect on the ultimate properties and performance of the E/C/CNTs nanocomposites. Based on possessing light weight and good modulus (of 31 GPa and 20.6 GPa at -90 °C and 80 °C, respectively), E/C/HCCNT can be considered as an interesting composite for structural applications by polymer engineers.

Keywords: carbon fiber, epoxy resin, multiwall carbon nanotube, dynamic mechanical properties.

Kompozyty żywicy epoksydowej z włóknami węglowymi wzmocnione karboksylowanymi nanorurkami węglowymi: dynamiczne badania mechaniczne

Streszczenie: Kompozyty żywicy epoksydowej wzmocnione jednokierunkowo włóknami węglowymi otrzymywano metodą prasowania na gorąco prepregów. Do kompozytów epoksydowo-węglowych (E/C) dodawano wielościenne nanorurki węglowe (MWCNT) oraz ich karboksylowane pochodne, z małą (LCCNT) lub dużą (HCCNT) zawartością grup karboksylowych. Wprowadzenie do osnowy E/C

¹⁾ University of Guilan, Department of Chemistry, Faculty of Sciences, P.O. Box 41335-1914, Rasht, Iran.

²⁾ Iran Polymer and Petrochemical Institute, Department of Composites, P.O. Box 14965-115, Tehran, Iran.

*) Author for correspondence; e-mail: radmm@guilan.ac.ir

jednorodnej dyspersji nanorurek węglowych (CNT), z uniknięciem tworzenia się pustych przestrzeni umożliwiło znaczną modyfikację właściwości kompozytów. Dynamiczna analiza mechaniczna DMA wykazała zwiększenie wartości temperatury zeszklenia (T_g) oraz modułu zachowawczego kompozytu E/C/HCCNT. Na podstawie równania Vogela-Fulchera-Tammanna (VFT) i Williama-Landela-Ferry'ego (WLF) oraz zasady superpozycji temperaturowo-czasowej (TTS) wyznaczono krzywe wiodące modułu zachowawczego. Pozorne energie aktywacji przekształceń molekularnych obliczono dla różnych wartości temperatury z zastosowaniem pochodnych numerycznych i równań WLF. Wyniki badań wskazują, że zawartość grup COOH w nanorurkach węglowych może mieć istotny wpływ na właściwości użytkowe nanokompozytów E/C/CNT. Ze względu na niewielką masę i duże wartości modułu sprężystości (odpowiednio 31 GPa i 20,6 GPa w temp. -90 °C i 80 °C) wytworzone kompozyty mogą być interesującym materiałem do zastosowań konstrukcyjnych.

Słowa kluczowe: włókno węglowe, żywica epoksydowa, wielościenna nanorurka węglowa, dynamiczne właściwości mechaniczne.

Fiber-reinforced composites typically offer excellent strength-to-weight ratios and cost-benefits that account for their increasing industrial applications. These composites, owing to their superior mechanical properties such as tensile strength, stiffness, and impact strength, have found remarkable applications in aerospace manufacture and in the industries requiring light but strong materials [1–4]. As a result of these interesting uses, a surge of investigations has been drawn towards fabrication of fiber composites with improved properties. In this line, mechanically improved fiber composites were obtained by addition of very thin platelets of alumina to a unidirectional carbon fiber/epoxy resin composite [5]. The strength of binding between the fibers and the epoxy resin matrix [6–8] is a crucial parameter governing the dynamic mechanical and many other properties of the composite and can be enhanced by adding carbon nanotubes (CNTs). It has also been proven that the characteristics of such nanocomposites deeply depend on the uniformity with which carbon nanotubes are dispersed in the epoxy matrix [9–11]. Ultrasonic agitation is an efficient homogenization technique commonly used to achieve better dispersion of carbon nanotubes. The quantity of carbon nanotubes and the functional groups anchored on their surface have great impacts on the mechanical properties of the composites made with epoxy resins. In support of this knowledge, Yoonessi showed that typical composites of epoxy resins and the CNTs which are densely grafted with linear primary diamines display improved storage shear moduli and glass transition temperatures in comparison to pure epoxy resins [7].

Carbon nanotubes are indeed the seamless cylindrical structure of graphene, so benefit from several prominent thermal [12], mechanical [13, 14] and electrical [15, 16] properties that account for their vast applications in various fields. Their application as reinforcing component in the production of polymer nanocomposites has received a lot of attention from both academic research and industries [17, 18]. An interesting feature of CNTs in nanocomposites is their low loading required to achieve favorite properties [19, 20].

Glass transition temperature (T_g) is an important parameter to characterize the intermolecular forces within amorphous composites and usually is measured by differential scanning calorimetry (DSC) and dynamic mechanical analysis [DMA, sometimes referred to as dynamic mechanical thermal analysis (DMTA) or thermomechanical analysis (TMA)]. Among these techniques, DMA typically gives the most reliable measures of transitions in polymers [21, 22]. Other methods such as DSC and TMA are not as sensitive as DMA, hence, for thermoset resins (highly crosslinked) T_g is often measured by DMA [23].

Here we explain an explicit contribution of multiwall carbon nanotubes (MWCNTs) in improving the mechanical properties of unidirectional carbon fiber reinforced epoxy resin composites (E/C). This study also goes further to reveal the impact of the average diameter and the surface carboxyl groups of MWCNTs on improving the mechanical property of the composites by strengthening the interfacial interactions between CNTs, carbon fibers, and epoxy resin.

Table 1. Carboxyl content, density and dimensions of the MWCNTs

Nanoparticle	Specific surface area m ² /g	Outer diameter nm	Length μm	True density g/cm ³	COOH wt %
Parent CNT	200	10–20	10–30	2.1	0.00
LCCNT	200	10–20	10–30	2.1	2.00
HCCNT	500	< 8	10–30	2.1	3.86

EXPERIMENTAL PART

Materials

Multiwall carbon nanotubes were obtained from the American Elements Co. USA (the characteristics of MWCNTs can be seen in Table 1). The unidirectional carbon fiber fabric, UD T300 with surface area of 200 g/m², was supplied by PMP Co. Iran and was used for the preparation of the composites. DGEBA epoxy resin (diglycidyl ether of bisphenol-A – Epikote 828, supplied by Momentive, USA) with the epoxy group content of 5.34 mmol/g was used as the matrix. The dicyandiamide (DICY) curing agent with melting point of 208–211 °C and average particle size of 150 nm was obtained from Mokarar Co. (Tehran, Iran). An imidazole accelerator, 1-methylimidazole (DY070), was purchased from Huntsman company.

Preparation of pure epoxy sample

A mixture of epoxy resin and the dicyandiamide (DICY) curing agent was prepared by mixing 7 phr of DICY with 100 phr of epoxy resin. Afterward, the prepared mixture was dispersed by a homogenizer at 3000 rpm for 60 min at room temperature. At the ending 3 min of the homogenization process, 1-methylimidazole (0.6 phr) was added as an accelerator to the mixture.

Preparation of mixtures of epoxy resin and MWCNT derivatives

DICY (7 phr) and the MWCNT (0.2 phr) were mixed with 100 phr of the epoxy resin by a glass rod, and then

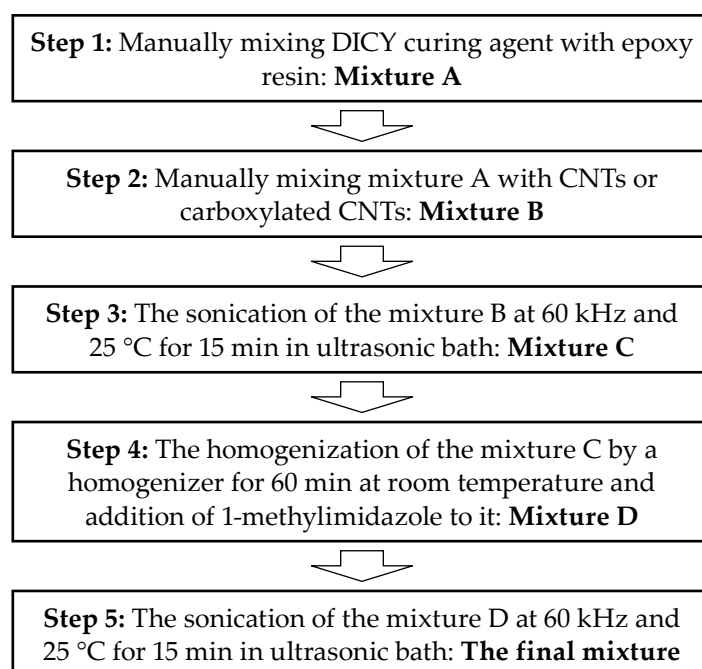
the prepared mixture was sonicated (60 kHz) at 25 °C in an ultrasonic bath for 15 min. Afterward, the prepared mixture was homogenized at 3000 rpm by a homogenizer for 60 min at room temperature. Then, 1-methylimidazole (0.6 phr) was added to the mixture and mixed for another 3 minutes by homogenizer. This final mixture was sonicated (60 kHz) at 25 °C for 15 min before being used for wetting the carbon fiber for the preparation of the preregs. The general protocol for preparation of the epoxy/MWCNT mixtures is shown in Scheme A. A homogenizer (Polytron, PT6100, Kinematica) was used to agitate the epoxy mixtures and achieve a homogeneous dispersion of CNT nanoparticles within these mixtures. The ultrasonic bath (LBS2 series, FALC instruments) was used for dispersion of CNTs in the mixtures.

Preparation of preregs

A sample of carbon fibers was impregnated with pure epoxy resin or a mixture of epoxy resin and the MWCNT, such that the ratio of fiber to resin was kept at 50 ± 2 wt % to assure all the fibers are impregnated homogeneously with the resin mixture. The impregnated single layer of the carbon fiber (prepreg) was ready for the next processing step of lay-up and curing *via* hot press to produce the composite and nanocomposite samples.

Preparation of composite samples

Nine plies of the carbon/epoxy preregs were laid up in a laminate orientation and the prepared 9-ply laminate was placed between two layers of teflon release film in an steel frame with the required thickness and then com-



Scheme A. Schematic representation of the procedure used for preparation of epoxy/CNTs mixtures

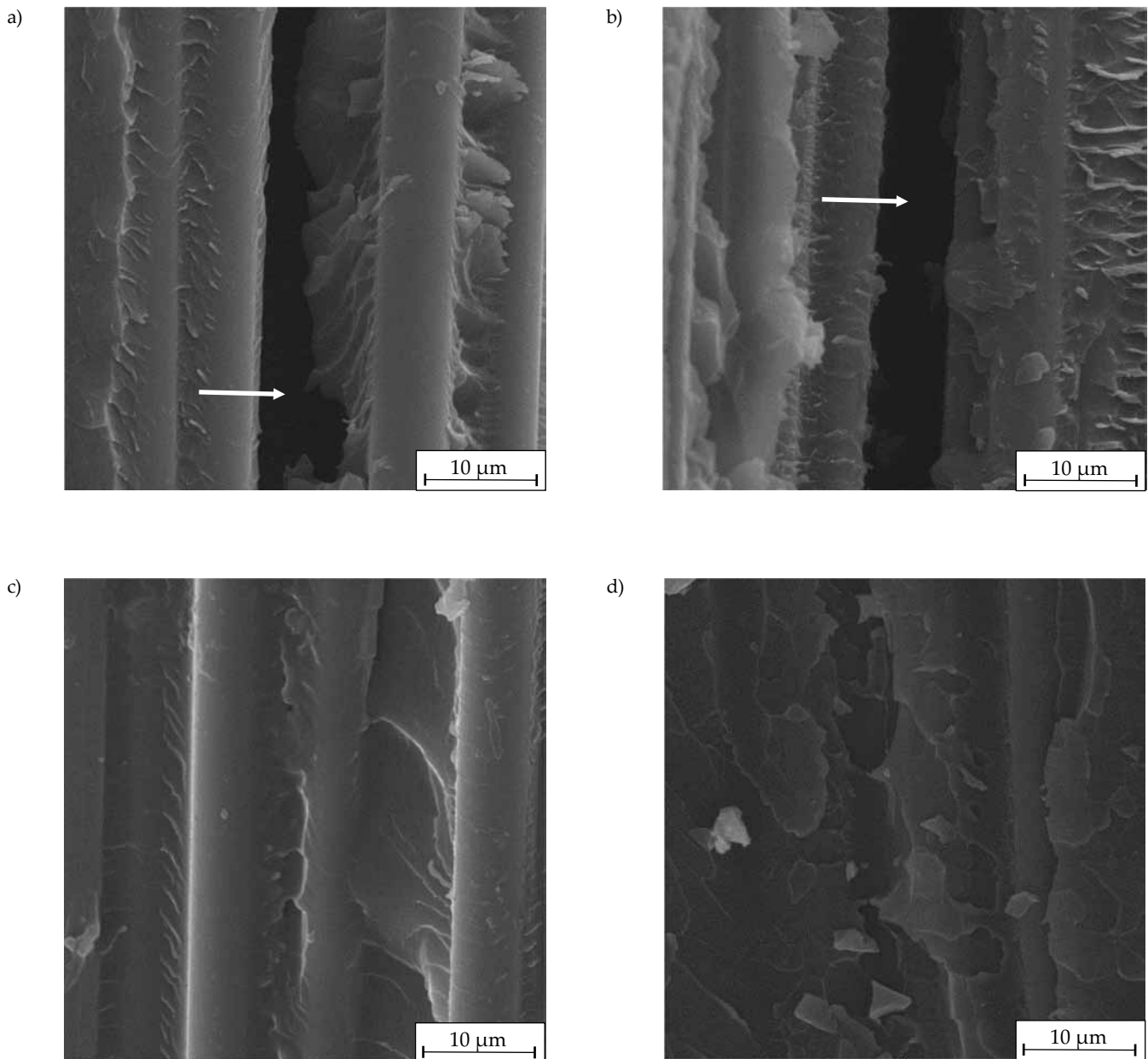


Fig. 1. SEM micrographs of the composites and nanocomposites: a) E/C, b) E/C/parent-CNT, c) E/C/LCCNT, d) E/C/HCCNT

pression-molded *via* hot pressing at 140 °C under 3 MPa for 1.5 h. After cooling the laminate to room temperature, samples with certain dimensions were cut with a diamond saw for the desired tests.

Methods of testing

The scanning electron microscopy (SEM) micrographs were taken by a VEGA/TESCAN scanning electron microscope (Czech Republic) to determine the morphology of the composite. Prior to placing into the microscope, the samples were coated with gold under vacuum by using a sputter coater (sputter coater, K450X, EMITECH, England). The voltage of the SEM filament was adjusted at 20 kV and several micrographs were obtained for each sample.

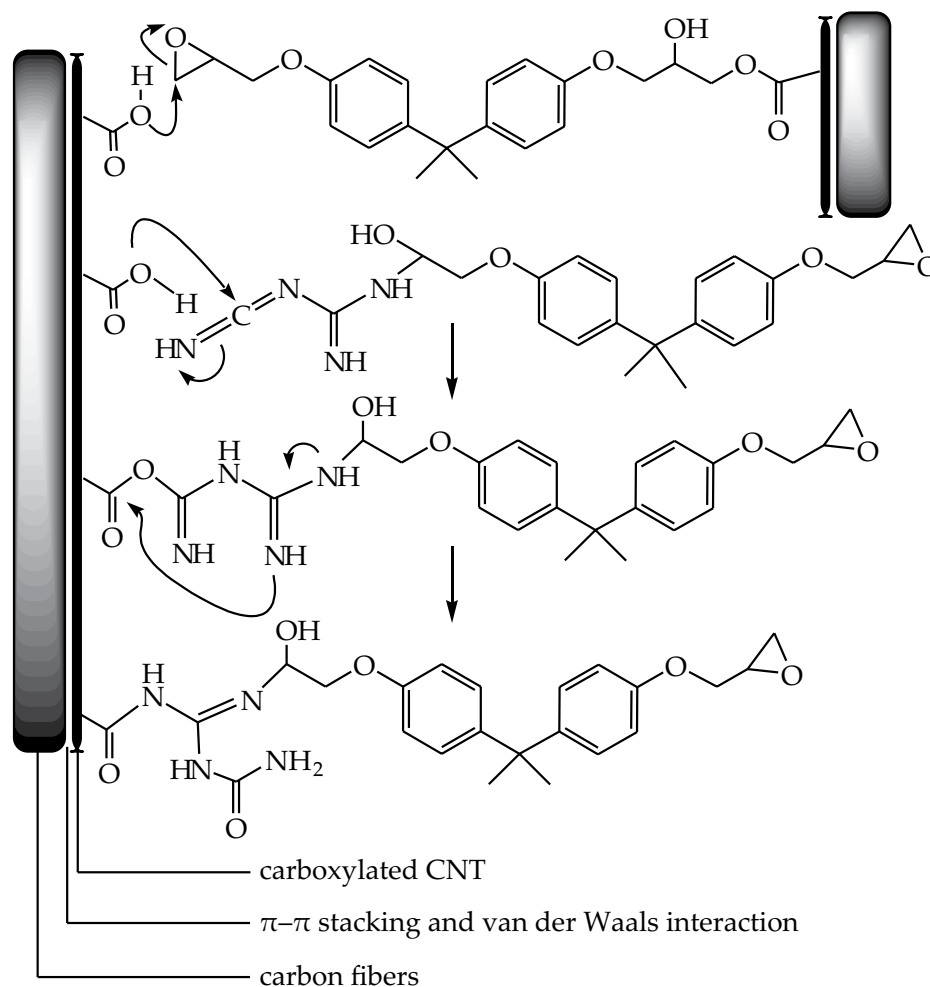
Dynamic mechanical analysis (DMA) was carried out in three point bending mode following the stan-

dard ASTM D5023, in multi frequency state by using a TT-DMA dynamic mechanical analyzer (Triton Technology Co England). The DMA experiments were conducted for the samples in the temperature range of -110 °C to 250 °C at a heating rate of 3 °C/min and five frequencies (0.1, 0.5, 1, 5 and 10 Hz).

RESULTS AND DISCUSSION

Scanning electron microscopy

Figure 1 exhibits the SEM micrographs of the E/C composites and their nanocomposites with MWCNT derivatives. As seen, these micrographs provide some insights into morphology and the dispersion of MWCNTs in the composites. The voids appeared in the micrograph of the pure E/C composite (free of MWCNT) indicate an in-



Scheme B. Schematic representation of typically important and expected interactions between carboxylated CNTs, epoxy resin and carbon fibers

complete bonding between the fibers and the epoxy matrix. Seki *et al.* similarly explained that the holes they observed in the SEM micrograph of jute fiber/epoxy/polyester composites arise from a weak adhesion between fibers and matrix [24]. These voids which imply less bonding between carbon fibers and epoxy resin become even greater when the composite is made from epoxy resin, carbon fibers, and unfunctionalized MWCNTs. On contrary, significant improvements in bonding between carbon fibers and epoxy matrix were obtained by application of carboxylated MWCNTs in fabrication of the composites. Two types of CNTs with different densities of surface carboxyl groups denoted as LCCNT (low carboxylated CNT) and HCCNT (higher carboxylated CNT) were employed to explore the impact of carboxyl groups on the interfacial bonding of carbon fibers to the epoxy resins. The SEM micrographs of the ternary composites fabricated from either LCCNTs or HCCNTs displayed no microvoids between the fibers and epoxy resin as an indication of improved bonding between the components. In addition, based on SEM micrographs, E/C/MWCNT was found to have a clearly rougher surface than E/C/LCCNT and E/C/HCCNT specimens. The higher roughness of E/C/MWCNT is due to non-proper dispersion of unfunc-

tionalized MWCNTs in the epoxy matrix that results in agglomeration of the CNTs. On contrary, the SEM micrographs of the E/C/LCCNT and E/C/HCCNT composites demonstrate increased uniformity and smoothness that can be ascribed to fine dispersion of the oxidized MWCNTs (containing COOH groups) in the polar epoxy matrix. Certainly, the better homogeneity and uniformity that is seen in the SEM micrograph of E/C/HCCNT in comparison to the two other composites and the fact that its micrograph does not have any void are attributed to the higher COOH content and also to the lower diameter of HCCNT in comparison with LCCNT and the parent MWCNT. The polar COOH groups of LCCNT and HCCNT significantly take part in dipole-dipole interactions as well as in hydrogen bonding and therefore make these nanoparticles more compatible than the unfunctionalized MWCNTs with epoxy resin. Thanks to possessing non-polar carbonaceous backbone and bearing polar COOH groups, the oxidized MWCNTs are amphiphilic materials. The amphiphilic nature of LCCNT and HCCNT allows them to establish non-polar and π - π stacking interactions with the carbon fibers and to exert in the same time dipole-dipole interactions with the polar groups of epoxy resin. Beside these cohesive forces, the carboxylated CNT particles are covalently

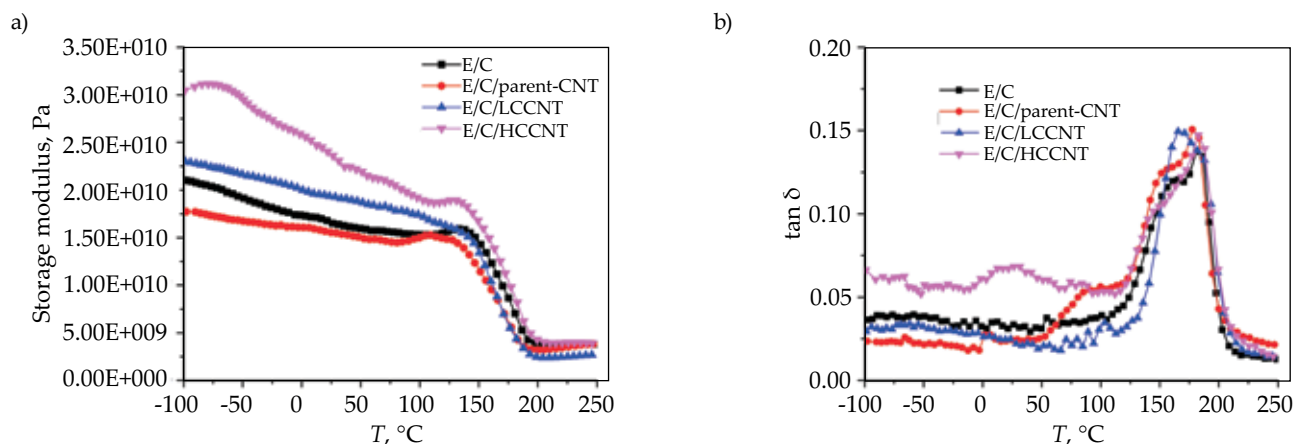


Fig. 2. DMA curves of the E/C composite and its CNT-nanocomposites at the test frequency of 10 Hz: a) storage modulus, b) $\tan \delta$

bound to the epoxy resin through the reaction of epoxy rings with carboxyl groups. In addition, the bonding reaction between epoxy resin and the carboxyl groups of CNTs are activated by DICY curing agent (Scheme B). Owing to formation of these bonds and interfacial interactions, the CNT particles gain better dispersion into epoxy resin that leads to a smooth appearance and uniform mechanical properties of the composite. Similar interfacial interactions were previously invoked by Peng who found from SEM studies that silylated CNTs are dispersed more uniformly in epoxy matrix [25].

Dynamic mechanical properties

Dynamic mechanical analyses (DMA) were taken to study the mechanical behavior of the composites. As is seen in Fig. 2, the storage modulus of the E/C composite is decreased by the addition of unfunctionalized MWCNTs, while the ternary composites (E/C/LCCNT and E/C/HCCNT) made by the addition of carboxylated CNTs have higher storage moduli than that of the binary E/C composite. The modulus of E/C/HCCNT is significantly higher than those of all other prepared composites. The decreased modulus of E/C/MWCNT can be explained in terms of interfacial adhesion reinforcing effects. Application of loads to the polymer composites is associated with stresses which transfer between the matrix and filler *via* the interface area and therefore the reinforcement effect depends on the interfacial adhesion. Under a given interfacial adhesion strength, reinforce of a polymeric composite is controlled by the interfacial area of the fillers [26]. It is noteworthy that the interfacial adhesion between polar epoxy resin and non-polar carbon fibers is weak and the load is not properly transferred between epoxy and carbon fibers. The non-polar area of the composite becomes even extended when unfunctionalized MWCNTs are added to the E/C composite whereupon the interfacial adhesion of epoxy resin weakens. However, on the other hand, the interfacial interaction between carboxylated CNTs and epoxy resin is relatively strong whereby

the load efficiently transfers between the epoxy resin and the carboxylated CNTs.

Effect of test frequency on the dynamic mechanical properties

In DMA measurements the storage modulus, loss modulus, and damping peaks depend largely on the test frequency, as increase of the frequency leads to increase of the storage modulus, especially at high temperatures, and shifts the damping ($\tan \delta$) peaks to higher temperatures [27]. It is known that when a material is subjected to a given constant stress its storage modulus will decrease over a period of time (frequency) because the material is molecularly rearranged to minimize the localized stresses. In other words, the modulus measurements that are taken over a short time (high frequency) result in higher values while the measurements done over longer times (low frequency) result in lower values of storage modulus [28].

Figures 3–6 exhibit the effect of test frequency on the storage modulus of the E/C composite and its nanocomposites with different MWCNTs. As can be seen, by increasing the frequency the peak of $\tan \delta$ shifts to higher temperatures. Noticeably, the modulus of E/C composite (Fig. 3) is increased in the range of 118 to 128 °C (with the peak at 123.6 °C) while similar increase for E/C/CNT (Fig. 4) shifts to lower temperatures and occurs at 90 to 108 °C (with the peak at ~99.5 °C). These peaks which appear as $\tan \delta$ shoulders above 90 °C can be attributed to changes in the fiber/epoxy interactions due to the new conformational rearrangements at higher temperatures. Another probable suggestion for appearance of these peaks arises from the voids between the carbon fibers and epoxy resin, as can be seen in the SEM micrographs of E/C and E/C/CNT, which allow more conformational flexibility and easier movements to the fibers and epoxy fragments at higher temperatures.

Figure 5 displays a smoothly decreasing modulus for the nanocomposite E/C/LCCNT with increase of temperature and does not show any peak at above 90 °C as is seen for E/C and E/C/CNT. This difference may be re-

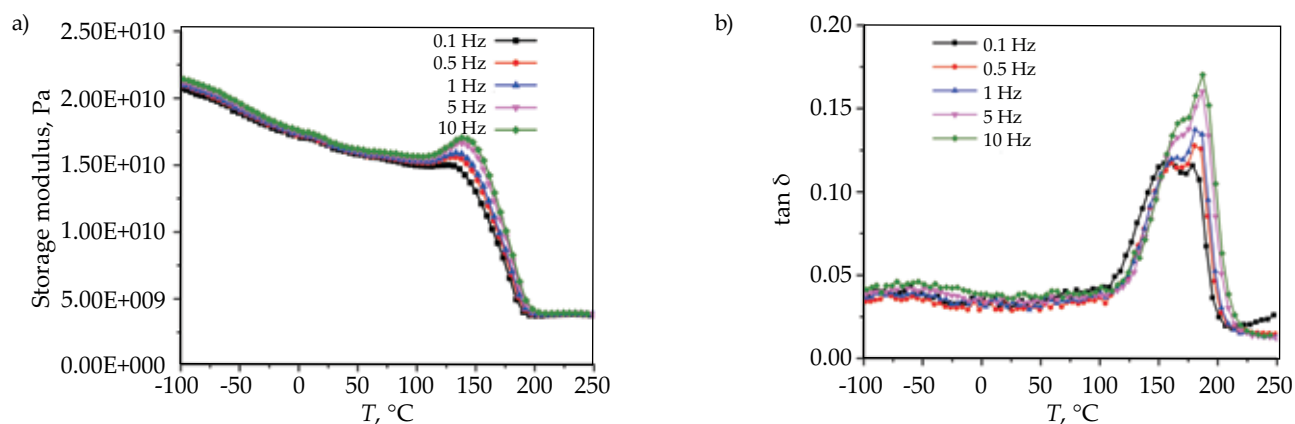


Fig. 3. Effect of test frequency on DMA curves of E/C composite at frequencies of 0.1, 0.5, 1, 5 and 10 Hz: a) storage modulus, b) $\tan \delta$

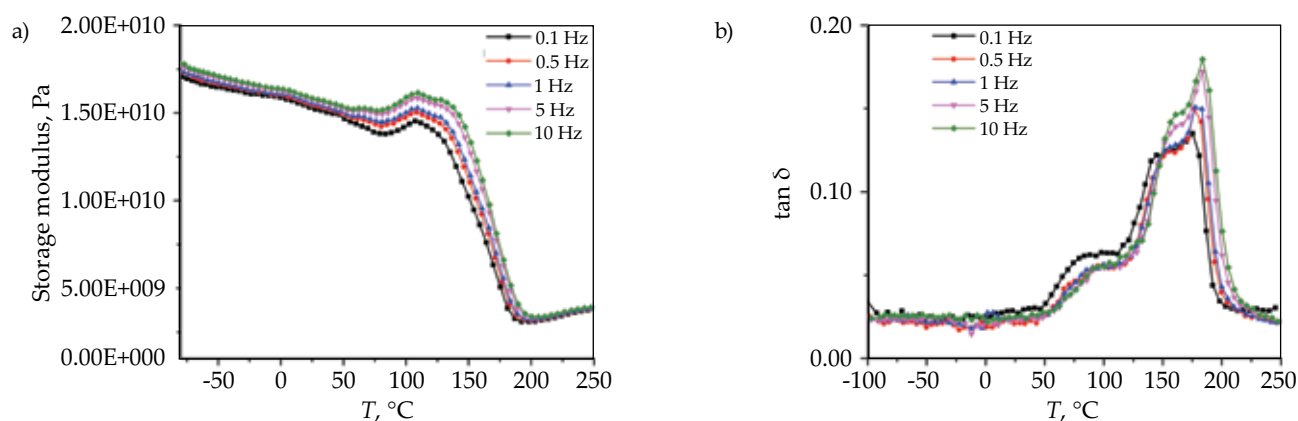


Fig. 4. Effect of test frequency on DMA curves of E/C/CNT nanocomposite at frequencies of 0.1, 0.5, 1, 5 and 10 Hz: a) storage modulus, b) $\tan \delta$

lated to the voids which appear in the SEM micrographs of E/C and E/C/CNT but do not exist within E/C/LCCNT. An alternative explanation for the observed modification is based on the limited local movements and conformational mobilities of epoxy resin due to efficient interactions with the carboxyl groups of CNTs.

In the case of E/C/HCCNT (Fig. 6) the modulus continuously decreases with rise of temperature and does

not show any peak above 90 °C or a sensible shoulder around the $\tan \delta$ peak. This exclusive behavior of E/C/HCCNT may be attributed to the thinner CNTs (~ 8 nm) in this composite which enable it to have different conformational movements with respect to the other composites, especially at higher temperatures.

The modulus values of the samples at typical temperatures (-90 °C and 80 °C) collected from the Figs. 3–6 were

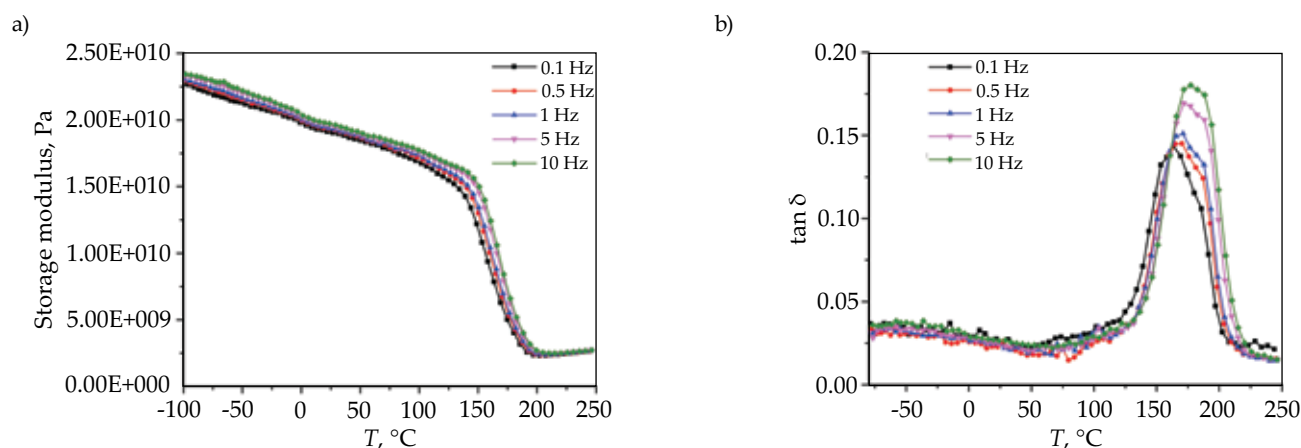


Fig. 5. Effect of test frequency on DMA curves of E/C/LCCNT nanocomposite at frequencies of 0.1, 0.5, 1, 5 and 10 Hz: a) storage modulus, b) $\tan \delta$

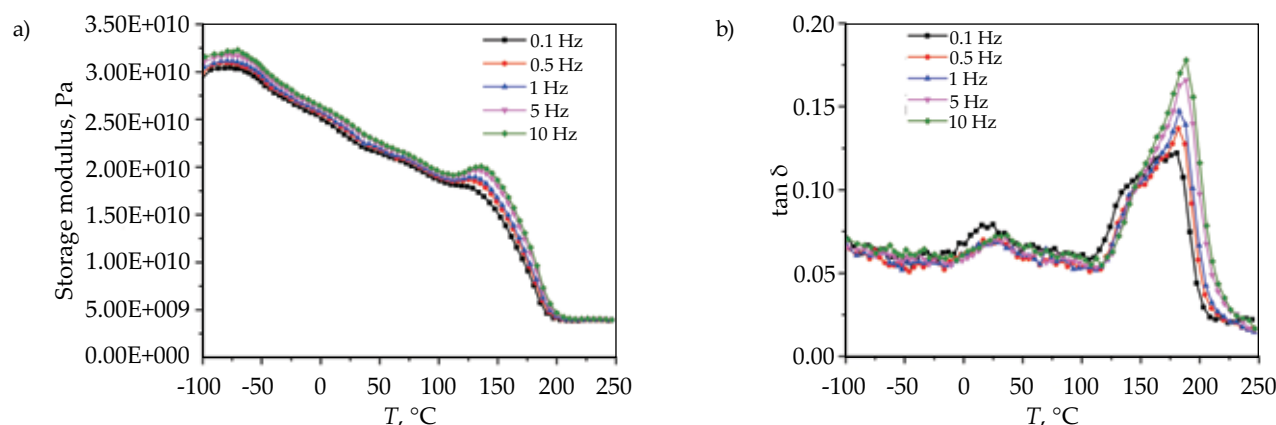


Fig. 6. Effect of test frequency on DMA curves of E/C/HCCNT nanocomposite at frequencies of 0.1, 0.5, 1, 5 and 10 Hz: a) storage modulus, b) $\tan \delta$

tabulated in Table 2, showing that at the various temperatures and frequencies the modulus of E/C/CNT is lower than that of E/C, while E/C/LCCNT and E/C/HCCNT have higher storage modulus values in comparison with E/C and E/C/CNT. On the basis of Table 2, it can be seen that the test frequency, temperature, polarity and density of the carboxyl groups present on the surface of the CNTs, and diameter of the CNTs are the important parameters affecting on DMA curves of the nanocomposites.

Glass transition temperature of the samples

Based on Fig. 2b, which displays the curve of $\tan \delta$ vs. temperature, one can find that the peak of $\tan \delta$ for E/C/CNT occurs at a lower temperature than for E/C/LCCNT and E/C/HCCNT. This shift can be assigned to the weak interfacial adhesion between the epoxy matrix and the unidirectional carbon fibers in the former composite. The fact that a similar curve for E/C/LCCNT gives a peak at a higher temperature than that of E/C/CNT is interpreted as greater compatibility of E/C matrix with LCCNT rather than with unfunctionalized CNTs. This compatibility is assigned to the amphiphilic nature of carboxylated CNTs that enables them to interact with epoxy matrix through dipole-dipole interaction of its COOH functional groups and with carbon fibers through π - π interaction of its carbonaceous backbone.

As expected, E/C/HCCNT displayed a $\tan \delta$ peak at relatively higher temperature than E/C/LCCNT and consequently a glass transition temperature (T_g) higher than those of two other ternary composites (E/C/CNT and E/C/LCCNT). No doubt, these improved properties are attributed to the higher COOH content (3.86 wt % compared to 0 and 2 wt % for the pristine MWCNT and LCCNT, respectively) and lower diameter of HCCNT (diameter < 8 nm compared to ~ 20 nm for the unfunctionalized MWCNT and LCCNT).

Master curves

The apparent segmental relaxation time is defined as the inverse of the angular frequency ($\tau = 1/\omega_{\max}$) at which the maxima of the loss modulus occur. Based on the loss modulus curves, the loss peaks shift to higher temperatures upon increasing frequency, meaning that relaxations occur faster at higher temperatures. The temperature dependence of relaxation time for the prepared samples can be described by the Vogel-Fulcher-Tammann (VFT) equation [29]:

$$\tau = \tau_0 \exp\left(\frac{B}{T - T_\infty}\right) \quad (1)$$

where: B is a material parameter relating to the apparent activation energy, T_∞ stands for the Vogel temperature

Table 2. Storage modulus of E/C and its nanocomposites at typical temperatures

Sample	$T, ^\circ\text{C}$	Storage modulus, GPa					
		Frequency, Hz					
		0.1	0.5	1.0	5.0	10.0	Ave.
E/C	-90	20.47	20.70	20.76	21.03	21.18	20.80
	80	15.31	15.45	15.52	15.70	15.86	15.57
E/C/CNT	-90	17.34	17.57	17.70	17.95	18.04	17.70
	80	13.86	14.39	14.65	15.18	15.46	14.70
E/C/LCCNT	-90	22.47	22.68	22.78	23.08	23.27	22.90
	80	17.64	17.72	17.84	18.18	18.25	17.90
E/C/HCCNT	-90	30.24	30.74	30.86	31.50	31.86	31.00
	80	20.12	20.44	20.50	20.81	20.99	20.60

displaying the point in which relaxation time diverges to infinity and the pre-exponent τ_0 corresponds to the relaxation time at infinite temperature. For each sample, τ was calculated by the frequency corresponding to the maximum point of the loss modulus peak. Afterward, the parameters B , T_∞ and τ_0 were calculated for all the samples by fitting the VFT equation on the raw data in MATLAB. The results were reported in Table 3.

On the basis of the time-temperature superposition principle, in order to evaluate the effects of MWCNT functionality and frequency on the dynamic mechanical properties of the E/C samples, time-temperature superposition principle (TTS) was used as a tool for making the master curves of the storage modulus by using multi-frequency data at a variety of temperatures. Figure 7 displays the storage modulus master curve for a reference temperature (T_{ref}) of 25 °C. In all the cases, the temperature dependent shift factor along the horizontal axis, α_t , has been determined according to the Williams-Landel-Ferry (WLF) equation as follows:

$$\log \alpha_t = \log \frac{\tau(T)}{\tau(T_{ref})} = \frac{C_1(T - T_{ref})}{C_2 + T - T_{ref}} \quad (2)$$

where: C_1 and C_2 are constant parameters for the polymer in T_{ref} and were calculated by using the VFT equation based on which $C_1 = B/2.303 (T_{ref} - T_\infty)$ and $C_2 = T_{ref} - T_\infty$ (Table 3). Upon calculation of $\log \alpha_t$ values in the corresponding temperature range of -100 to 250 °C and $T_{ref} = 25$ °C for each sample, the logarithmic plots of the storage modulus against the angular frequency, ω , were

produced. It is obvious from Eq. 1 that if $T > T_{ref}$, $\alpha_t > 0$ and then $T < T_{ref}$, $\alpha_t < 0$.

From the master curves, it can be found that increasing the angular frequency (ω) leads to an increase in the storage modulus, *i.e.*, the higher frequency means shorter times of applying the load to the samples and decreasing the loading time leads to a higher modulus. Moreover, these figures confirm the higher storage modulus of E/C/HCCNT in comparison to other samples. Because of having the highest COOH content, HCCNT induces the highest reinforcing effect, among the CNT samples, and in turn the highest modulus in E/C/HCCNT.

The shift factor ($\log \alpha_t$) which represents the basic effect of temperature on the material's viscoelastic properties is shown in Fig. 8. It can be seen that the shift factor values decrease with increasing the temperature.

Apparent activation energy

Apparent activation energy (E_α) in the glass transition region depends on the energy required for promotion of the initial movements of some molecular segments. Higher activations require higher amounts of energy for initiation of polymer chain movements. E_α can be calculated from the temperature dependence of storage (E') and loss (E'') moduli by numerical derivative and WLF equations. E_α for E/C composite and its nanocomposites were calculated, based on the numerical derivative (Eq. 3) and WLF (Eq. 4) equations, and then plotted at different temperatures *via* the following expressions (Fig. 9) [30]:

Table 3. Fit parameters of VFT and WLF equations for relaxation data of the prepared E/C composite and its corresponding nanocomposites

Sample	Frequency Hz	τ , s	B , K	T_{ref} , K	T_∞ , K	C_1	C_2 , K	τ_0 , s
E/C	0.1	1.592	396.6	298.15	433.7	-1.270	-135.55	5.29E-10
	0.5	0.318	396.6	298.15	433.7	-1.270	-135.55	5.29E-10
	1	0.159	396.6	298.15	433.7	-1.270	-135.55	5.29E-10
	5	0.032	396.6	298.15	433.7	-1.270	-135.55	5.29E-10
	10	0.016	396.6	298.15	433.7	-1.270	-135.55	5.29E-10
E/C/parent-CNT	0.1	1.592	418.3	298.15	425.9	0.00	-127.75	1.08E-08
	0.5	0.318	418.3	298.15	425.9	0.00	-127.75	1.08E-08
	1	0.159	418.3	298.15	425.9	0.00	-127.75	1.08E-08
	5	0.031	418.3	298.15	425.9	0.00	-127.75	1.08E-08
	10	0.015	418.3	298.15	425.9	0.00	-127.75	1.08E-08
E/C/LCCNT	0.1	1.592	402.9	298.15	423.0	-1.399	-125.05	4.13E-13
	0.5	0.318	402.9	298.15	423.0	-1.399	-125.05	4.13E-13
	1	0.159	402.9	298.15	423.0	-1.399	-125.05	4.13E-13
	5	0.031	402.9	298.15	423.0	-1.399	-125.05	4.13E-13
	10	0.015	402.9	298.15	423.0	-1.399	-125.05	4.13E-13
E/C/HCCNT	0.1	1.592	390.4	298.15	436.3	-1.227	-138.15	3.09E-10
	0.5	0.318	390.4	298.15	436.3	-1.227	-138.15	3.09E-10
	1	0.159	390.4	298.15	436.3	-1.227	-138.15	3.09E-10
	5	0.031	390.4	298.15	436.3	-1.227	-138.15	3.09E-10
	10	0.015	390.4	298.15	436.3	-1.227	-138.15	3.09E-10

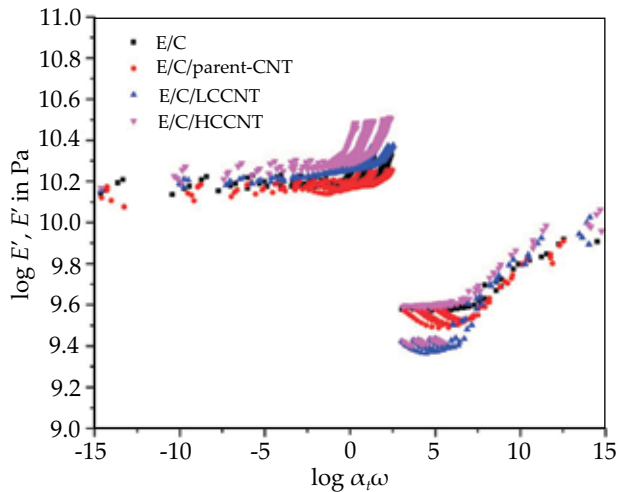


Fig. 7. Master curves of storage modulus at reference temperature 0 °C for E/C composite and its CNT-nanocomposites; $\log \alpha_t$ used in TTS are from WLF fit

$$E_{\alpha} = 2.303 R \frac{d \log \alpha_T}{d(\frac{1}{T})} \quad (3)$$

$$E_{\alpha} = 2.303 R \frac{C_1 C_2 T^2}{(C_2 + T - T_{ref})^2} \quad (4)$$

where: $R = 8.314 \text{ J/(K} \cdot \text{mol)}$ denotes the gas constant and α_T refers to the shift factor. Moreover, C_1 and C_2 , which are tabulated in Table 3, are constant parameters at $T_{ref} = 25 \text{ }^{\circ}\text{C}$. As is seen in Fig. 9, the apparent activation energy (E_{α}) values are decreased for all the samples after $\sim 150 \text{ }^{\circ}\text{C}$ by increasing the applied temperature. However, on contrary, these energies increase as temperature is raised within the range of 100–150 °C. It is noteworthy that this range corresponds to similar temperatures in the DMA curves of the composites in which the storage modulus is increased. The increase of activation energy in these temperatures can be attributed to new interactions and rearrangements of the polymeric chains. This behavior is not surprising since the amount of energy required for the polymer chain motions decreases at increased temperatures. Notably, the two sets of data obtained on the

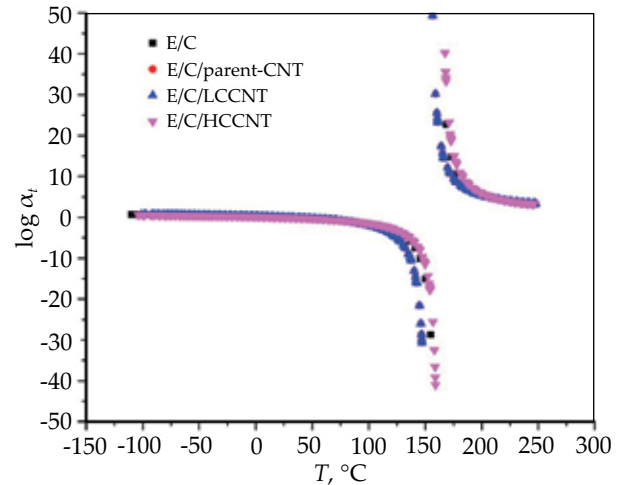


Fig. 8. Temperature dependence of the shift factor α_t for E/C composite and its CNT-nanocomposites

basis of the numerical derivative and WLF equations are in good agreement with each other, confirming that the calculated data for apparent activation energy of all the samples are valid over the temperatures considered.

CONCLUSIONS

Samples of pure epoxy resin and its homogenized mixtures with MWCNTs or carboxylated MWCNTs were prepared *via* mixing by using a homogenizer working at 3000 rpm. A given amount of unidirectional carbon fibers was impregnated with the prepared epoxy mixtures. Afterward, 9-ply laminates of the impregnated carbon fibers (prepregs) were cured *via* hot pressing to prepare the nanocomposites. The SEM micrographs of epoxy/carbon fiber composite showed micro-voids which are suspected to originate from the weak adhesion at epoxy/fiber (E/C) interface. These micro-voids even increase when the composites are made from E/C and unfunctionalized MWCNTs. Low carboxylated MWCNTs (LCCNTs) and high carboxylated MWCNTs (HCCNTs) were also used for the preparation of

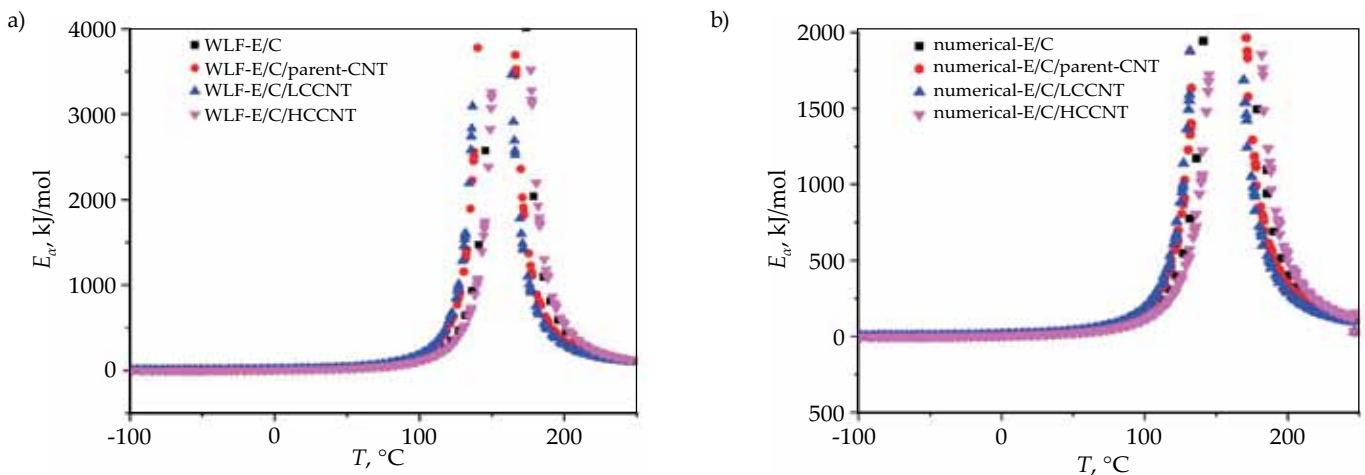


Fig. 9. Temperature dependence of the apparent activation energy for α -relaxation processes in E/C composite and its nanocomposites: a) WLF equation, b) numerical derivative equation

similar composites. In the micrographs of E/C/LCCNT and E/C/HCCNT specimens the micro-voids were completely disappeared. Notably, the SEM micrograph of E/C/HCCNT has a more uniform appearance than E/C/LCCNT. This difference seems to be arisen from the higher COOH content and lower diameter of HCCNT as compared to that of unfunctionalized MWCNT and LCCNT. Beside intrinsic π - π stacking and van der Waals attractions with carbon fibers, the oxidized MWCNTs with higher COOH contents are able to establish dipole-dipole interactions with the matrix of epoxy resin and so are compatible with both carbon fibers and epoxy resins. As a consequence of these compatibilities HCCNTs are more homogeneously dispersed with respect to unfunctionalized MWCNTs and LCCNTs in the mixture of epoxy resin and carbon fibers to make a smoother composite. The DMA studies showed that the nanocomposites of E/C and COOH-containing MWCNT have higher T_g and storage moduli than pure E/C and E/C/MWCNT composites. These improvements can be ascribed to stronger interaction of LCCNT and especially HCCNT with epoxy resin of the E/C matrix. In addition, this study displays that temperature, test frequency, and the COOH content of CNTs are the main factors controlling the storage moduli and the DMA curves of the prepared composites. Calculations based on time-temperature superposition principle showed that E' (storage modulus) increases upon increasing the angular frequency (master curve of storage modulus) and also the shift factor values decrease with increasing the temperature. The apparent activation energies of molecular rearrangements were also determined and their plots indicated that these values decrease by increasing the temperature.

REFERENCES

- [1] Indicula M., Boudenne A.: *Composites Science and Technology* **2006**, 66, 2719.
<http://dx.doi.org/10.1016/j.compscitech.2006.03.007>
- [2] Assael M.T., Antoniadis K.D., Tzetzis D.: *Composites Science and Technology* **2008**, 68, 3178.
<http://dx.doi.org/10.1016/j.compscitech.2008.07.019>
- [3] Kumlutas D., Tavman I.H., Turhan-Çoban M.: *Composites Science and Technology* **2003**, 63, 113.
[http://dx.doi.org/10.1016/S0266-3538\(02\)00194-X](http://dx.doi.org/10.1016/S0266-3538(02)00194-X)
- [4] Kim D., Chung I., Kim G.: *Fibers and Polymers* **2013**, 14, 2141. <http://dx.doi.org/10.1007/s12221-013-2141-9>
- [5] Sherman D., Lemaitre J., Leckie F.: *Acta Metallurgica et Materialia* **1995**, 43, 4483.
[http://dx.doi.org/10.1016/0956-7151\(95\)00136-J](http://dx.doi.org/10.1016/0956-7151(95)00136-J)
- [6] Godara A., Gorbatiikh L., Kalinka G. *et al.*: *Composites Science and Technology* **2010**, 70, 1346.
<http://dx.doi.org/10.1016/j.compscitech.2010.04.010>
- [7] Yoonessi M., Lebron-Colon M., Scheiman D. *et al.*: *ACS Applied Materials & Interfaces* **2014**, 6, 16 621.
<http://dx.doi.org/10.1021/am5056849>
- [8] Islam M.E., Mahdi T.H., Hosur M.V. *et al.*: *Procedia Engineering* **2015**, 105, 821.
<http://dx.doi.org/10.1016/j.proeng.2015.05.078>
- [9] Piesowicz E., Irska I., Bryll K. *et al.*: *Polimery* **2016**, 61, 24.
<http://dx.doi.org/10.14314/polimery.2016.024>
- [10] Chen B., Chen J., Li J. *et al.*: *Chinese Journal of Polymer Science* **2017**, 35, 446.
<http://dx.doi.org/10.1007/s10118-017-1911-z>
- [11] Mir Mohammad Alavi N., Yaghoubi A.: *Polimery* **2014**, 59, 776. <http://dx.doi.org/10.14314/polimery.2014.776>
- [12] Kim P., Shi L., Majumdar A. *et al.*: *Physical Review Letters* **2001**, 87, 215 502.
<http://dx.doi.org/10.1103/PhysRevLett.87.215502>
- [13] Treacy M.M.J., Ebbesen T.W., Gibson J.M.: *Nature* **1996**, 381, 678. <http://dx.doi.org/10.1038/381678a0>
- [14] Wong E.W., Sheehan P.E., Lieber C.M.: *Science* **1997**, 277, 1971. <http://dx.doi.org/10.1126/science.277.5334.1971>
- [15] Wildoer J.W.G., Venema L.C., Rinzler A.G. *et al.*: *Nature* **1998**, 391, 59.
<http://dx.doi.org/10.1038/34139>
- [16] Odom T.W., Huang J.L., Kim P. *et al.*: *Nature* **1998**, 391, 62. <http://dx.doi.org/10.1038/34145>
- [17] Coleman J.N., Khan U., Blau W.J. *et al.*: *Carbon* **2006**, 44, 1624. <http://dx.doi.org/10.1016/j.carbon.2006.02.038>
- [18] Thostenson E.T., Chou T.W.: *Carbon* **2006**, 44, 3022.
<http://dx.doi.org/10.1016/j.carbon.2006.05.014>
- [19] Gojny F.H., Wichmann M.H.G.: *Composites Science and Technology* **2005**, 65, 2300.
<http://dx.doi.org/10.1016/j.compscitech.2005.04.021>
- [20] Hubert P., Ashrafi B., Adhikari K. *et al.*: *Composites Science and Technology* **2009**, 69, 2274.
<http://dx.doi.org/10.1016/j.compscitech.2009.04.023>
- [21] Goertzen W.K., Kessler M.R.: *Composites Part B: Engineering* **2007**, 38, 1.
<http://dx.doi.org/10.1016/j.compositesb.2006.06.002>
- [22] Wolfrum J., Ehrenstein G., Avondet M.: *Journal of Thermal Analysis and Calorimetry* **1999**, 56, 1147.
<http://dx.doi.org/10.1023/A:1010109129224>
- [23] Pascault J.P., Sautereau H., Verdu J. *et al.*: "Thermosetting polymers", Marcel Dekker Inc., New York 2002.
- [24] Seki Y.: *Materials Science and Engineering A* **2009**, 508, 247. <http://dx.doi.org/10.1016/j.msea.2009.01.043>
- [25] Ma P.C., Kim J.K., Tang B.Z.: *Composites Science and Technology* **2007**, 67, 2965.
<http://dx.doi.org/10.1016/j.compscitech.2007.05.006>
- [26] Turcsanyi B., Pukanszky B., Tudos F.: *Journal of Materials Science Letters* **1988**, 7, 160.
<http://dx.doi.org/10.1007/BF01730605>
- [27] Pothan L.A., Oommen Z., Thomas S.: *Composites Science and Technology* **2003**, 63, 283.
[http://dx.doi.org/10.1016/S0266-3538\(02\)00254-3](http://dx.doi.org/10.1016/S0266-3538(02)00254-3)
- [28] Murayama T.: "Dynamic mechanical analysis of polymeric materials", 2th ed., Elsevier, Amsterdam 1978.
- [29] Chehrazi E., Qazvini N.T.: *Iranian Polymer Journal* **2013**, 22, 613. <http://dx.doi.org/10.1007/s13726-013-0160-4>
- [30] Shamsi R., Mir Mohamad Sadeghi G., Asghari G.H.: *Polymer Composites*, available online 27 July 2016.
<http://dx.doi.org/10.1002/pc.24155>